

# Cellular compartments cause multistability in biochemical reaction networks and allow cells to process more information

Heather A. Harrington<sup>1\*</sup>, Elisenda Feliu<sup>2\*</sup>, Carsten Wiuf<sup>2†</sup>, and Michael P.H. Stumpf<sup>13†</sup>

<sup>1</sup>Theoretical Systems Biology, Division of Molecular Biosciences, Imperial College London, Wolfson Building, London, SW7 2AZ, UK

<sup>2</sup>Department of Mathematical Sciences, University of Copenhagen, Universitetsparken 5, 2100 Copenhagen, Denmark

<sup>3</sup>Institute of Chemical Biology, Imperial College London

<sup>†</sup>To whom correspondence should be addressed: wiuf@math.ku.dk, m.stumpf@imperial.ac.uk

\*Joint first authors

February 21, 2022

## Abstract

Many biological, physical, and social interactions have a particular dependence on where they take place. In living cells, protein movement between the nucleus and cytoplasm affects cellular response (i.e., proteins must be present in the nucleus to regulate their target genes). Here we use recent developments from dynamical systems and chemical reaction network theory to identify and characterize the key-role of the spatial organization of eukaryotic cells in cellular information processing. In particular the existence of distinct compartments plays a pivotal role in whether a system is capable of multistationarity (multiple response states), and is thus directly linked to the amount of information that the signaling molecules can represent in the nucleus. Multistationarity provides a mechanism for switching between different response states in cell signaling systems and enables multiple outcomes for cellular-decision making. We find that introducing species localization can alter the capacity for multistationarity and mathematically demonstrate that shuttling confers flexibility for and greater control of the emergence of an all-or-none response.

*Keywords: chemical reaction networks, MAPK, mass-action kinetics, cellular information processing, spatial localization*

## Introduction

Cells constantly have to adapt and respond to their environment. In single-celled organisms those cells least well adjusted to their surroundings will tend to contribute less to future generations than cells that are able to assimilate better or more quickly to changing circumstances. In multi-cellular organisms, aberrant response of individual cells to environmental or physiological cues may result in developmental anomalies or disease. The way in which cells respond to external signals, process them and act upon them is thus intimately and inextricably linked to an organism's fate [1, 2]; and in the long-term evolution will shape the molecular machinery underlying cellular decision making processes [3, 4].

One central aspect of biological information processing is the mapping of environments onto intracellular states given by the abundances of the molecular species (proteins, mRNAs, metabolites etc) under consideration. In this processing of information one or more environmental variables need to be represented in a way that facilitates the appropriate response. Continuous and discrete representations have

been reported, and it is easy to see how an increased number of states will start to mimic the “analog” nature of continuously varying states; here, of course, we are typically only interested in stable states. A simple “on/off” switch, for example, is a binary representation or response mechanism; this behavior is particularly interesting if there is a regime of conditions where the system can populate either state. In this case we speak of a bistable switch; outside this regime we only find a single state for the system. More generally we speak of multistability if more than two stable states are obtainable simultaneously.

The number of states in which a cell can be at any given time is linked to the flexibility in its decision making [5]. If only one state is accessible (and stable) then there is obviously no room for “choice” (even if such choices are made by random processes) and any cell-to-cell variability will derive from intrinsic or extrinsic sources of noise which will broaden out the population behavior around such stable states. For bi- and multistable systems, however, cell-to-cell variability may to a large extent be explained in terms of different states being occupied by different cells (even though they are genetically identical). From such variation different cell fates may be differentially accessible and hence understanding the causes of multistability in signal transduction will have ramifications across many areas of modern biology, notably stem-cell biology and regenerative medicine.

One canonical class of biological systems exhibiting multistability are protein kinase cascades that involve multiple phosphorylation of a substrate [6]. Mitogen activated protein kinase (MAPK) cascades are the most popular exponents of this type of system [7]. Depending on the mechanism of (de-)phosphorylation bistability in such systems can arise [8], which would give such systems the ability to use different levels of phosphorylation of the final substrate, *e.g.*, Erk. This has been an area of growing activity in recent years, because of the important role MAPKs play in cell-fate determination.

The ultimate function of Erk is to initiate a host of transcriptional responses. To fulfill such a function, activated Erk has to shuttle into the nucleus and a growing body of recent work is paying attention to such spatial aspects of signal transduction [9–11]. Here we show that this spatial organization [12] of signal transduction processes plays a pronounced role in increasing the “computational space” available to cells. Interestingly, the same effect has been observed at the onset of mitosis [13]. Very much like the physical `Address space` in a computer processor [14], the biological equivalent is influenced by the (bio-)physical organization of such systems. And here we show how the compartmentalization increases the number of stable states that can become simultaneously accessible, conferring greater flexibility and plasticity to such systems. Importantly, spatial organization can induce multistability into systems that otherwise would be mono-stable, as well as (sometimes considerably) increase the number of states in systems where the presence of multiple-phosphorylation sites would already give rise to multistable behavior.

This work complements the findings in [15] by providing a detailed mathematical analysis focused on the Erk shuttling mechanisms. Identifying whether a system exhibits multistable behavior or not, is however, challenging. This type of behavior may be limited to small regions of parameter space and in high-dimensional spaces (our systems considered here have 20 and 36 parameters (reaction rate constants), respectively) it is likely not detectable by simulation or random search of the parameter space; instead other approaches are called for. Here we base our arguments on a set of generalizable heuristics that conclusively assert or reject a system’s capacity for multistability, and which allow us to identify and delineate multi- and monostable regions in parameter space.

## 1 Results

We introduce and illustrate this framework for a basic building block of many signal transduction systems that for spatially homogeneous systems is guaranteed to be monostable. A one-site phosphorylation cycle — other post-translational modifications can, of course also be considered — consists of the reversible modification of a substrate  $S$  into its phosphorylated form  $S^*$ . Phosphorylation and dephosphorylation are

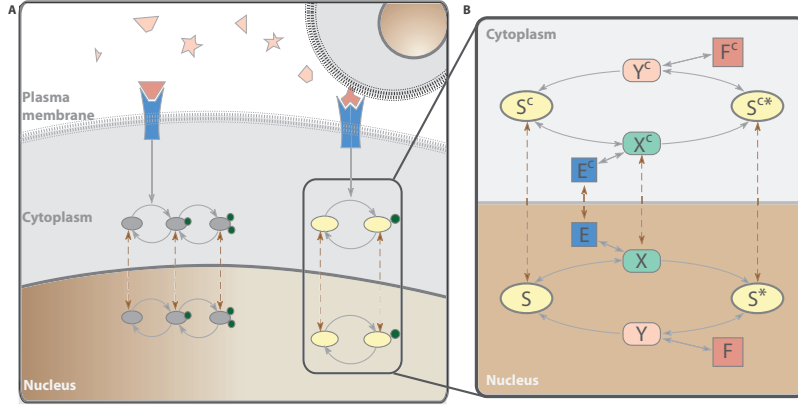
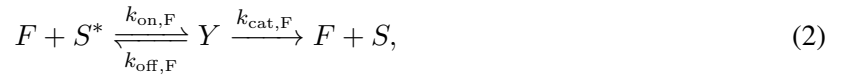
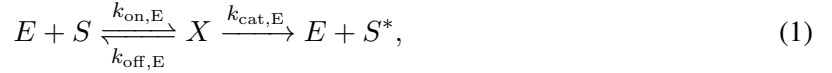


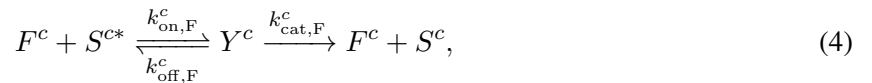
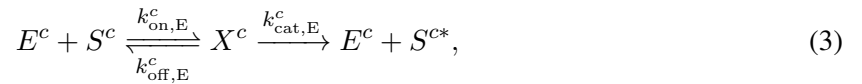
Figure 1: Spatial signaling schematic. (A) Cells require movement of molecular species within the plasma membrane, cytoplasm, nucleus and more cell locations to turn genes on or off and ultimately induce a response. (B) One-site phosphorylation/dephosphorylation in two compartments, cytoplasm and nucleus. Molecular species: unphosphorylated substrate ( $S$ ), kinase ( $E$ ), substrate-kinase complex ( $X$ ), phosphorylated substrate ( $S^*$ ), phosphatase ( $F$ ), phosphatase- phosphorylated substrate complex ( $Y$ ) and superscript  $c$  denotes species in the cytoplasm and all others are in the nuclear compartment. Kinase and substrate total abundances ( $E_{tot}, S_{tot}$ ) are globally conserved, while phosphatase abundances are conserved within each compartment ( $F_{tot}, F_{tot}^c$ ).

enzymatically catalyzed by  $E$  (kinase) and  $F$  (phosphatase), respectively, through a standard Michaelis-Menten mechanism involving the formation of intermediate complexes  $X, Y$ :

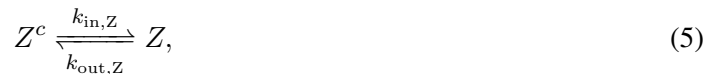


where  $k_*$  denote the reaction rate constants. Endowed with mass-action kinetics, this cycle is monostable [16, 17].

Now suppose we learn that these enzymatic reactions can both occur in both the nucleus and the cytoplasm (Fig. 1) and we therefore include the reactions in the cytoplasm (denoted by the  $c$  superscript)



as well as shuttling reactions between cytoplasm and nucleus <sup>1</sup>



for the species  $Z$  of the one-site phosphorylation cycle that shuttle into the nucleus at rate  $k_{in,Z}$  and out at  $k_{out,Z}$ . Total kinase, phosphatase and substrate abundances are constant for each compartment or globally depending on which species are allowed to shuttle between compartments. Here we use variation in the

<sup>1</sup>We remain in a regime where compartmental models are appropriate and where we do not have to model diffusive motion using reaction-diffusion equations. This is appropriate for all cases where transport across a membrane is rate-limiting.

amount of active kinase to model how external stimuli are processed and use the substrate state to capture the effects of stimuli.

The species abundances are modeled by a system of ordinary differential equations, which we analyze to determine if the system can exhibit multiple steady states (multistationarity) or not. This analysis employs a suite of different mathematical techniques, including the Jacobian injectivity criterion and recent developments from chemical reaction network theory [18–21] (see the Appendix for details). When multistationarity can occur we thereby obtain corresponding values of the rate constants and the steady states. Further, we delimit regions of the parameter space that contain all sets of rate constants that give rise to multistationarity.

## 1.1 Analytic conditions for multistability

Armed with these tools we establish that multistationarity cannot occur if only one species shuttles; if two species shuttle, then only the combinations  $\{X, S^*\}$  or  $\{S, Y\}$  can induce multistationarity for certain total amounts and rates; and increasing the number of species that shuttle maintains multistationarity (see the Appendix for a full description of the sets of shuttling species inducing multistationarity). The fact that the model includes the formation of at least one of the intermediate complexes  $X, Y$  (and hence some form of sequestration) is critical for the creation of multistationarity.

In particular, multistationarity occurs if the species  $E, S, X, S^*$  are allowed to shuttle (Fig. 1B). We choose to study this system in detail because it corresponds to a spatial model of a simplified one-site MAPK model system [9, 22] that is strictly monostable.

If the shuttling rates fulfill

$$k_{in,X} \geq k_{in,E} \quad k_{out,X} \geq k_{out,E} \quad k_{in,S} \geq k_{in,S^*} \quad k_{out,S} \geq k_{out,S^*}, \quad (6)$$

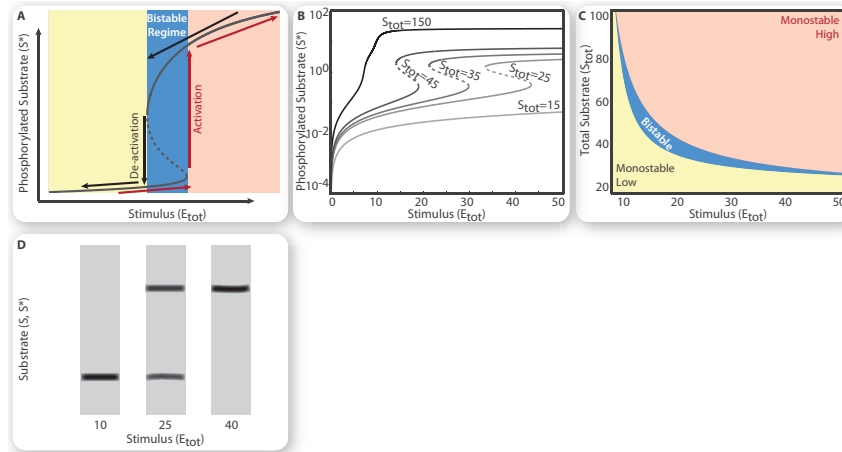


Figure 2: Bistability in one-cycle localization model. Rate constants and total amounts are given in the Appendix. (A) Steady state curve of phosphorylated nuclear substrate ( $S^*$ ) shows bistability and hysteresis as a function of stimulus (total kinase  $E_{tot}$ ). Stable states, solid lines; unstable state, dashed lines. Activation (phosphorylation) and deactivation (dephosphorylation) switches discontinuously from one stable branch to another at different stimulus thresholds, corresponding to the boundary values of the bistable regime (blue region). (B) Steady state curves of  $S^*$  as a function of stimulus ( $E_{tot}$ ) at varying amounts of total substrate ( $S_{tot}$ ). (C) Steady state diagram identifying the regions of parameter space supporting monostability (yellow, orange) or bistability (blue) as a function of the total amounts of kinase ( $E_{tot}$ ) and substrate ( $S_{tot}$ ). (D) Theoretical western blot of bistable (two bands) or monostable (one band) behavior depending on dose of stimulus.

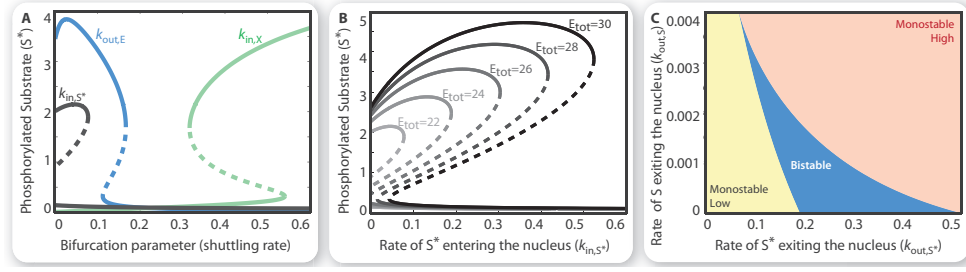


Figure 3: Effects of shuttling in the one-site localization model. Rate constants and total amounts as in Fig. 2. (A) Three steady state curve behaviors of phosphorylated nuclear substrate ( $S^*$ ) as shuttling are varied: high to low reversible bistability (blue,  $k_{out,E}$ ), low to high reversible bistability (green,  $k_{in,X}$ ), high to low irreversible bistability (black,  $k_{in,S^*}$ ). (B) Steady state curves of phosphorylated nuclear substrate ( $S^*$ ) as a function of the rate constant of  $S^*$  shuttling into the nucleus ( $k_{in,S^*}$ ) at varying amounts of stimulus ( $E_{tot}$ ). (C) Steady state diagram identifying the regions of parameter space supporting monostability (yellow, orange) or bistability (blue) as a function of  $k_{out,S}$  and  $k_{out,S^*}$ .

then multistationarity cannot occur even for the spatial model, whatever total amounts and reaction constants within each cycle (see the Appendix). The shuttling rates are paired for species  $E, X$  and species  $S, S^*$  and therefore a necessary condition for multistationarity is that either  $X$  moves in or out of the nucleus slower than the kinase,  $E$ ; or alternatively that  $S$  shuttles more slowly than its active form,  $S^*$ .

We next home in on a set of biologically plausible rate constants and total abundances for which the system has three steady states, two of which are stable. We find that at low and high stimulus doses (*i.e.*, total kinase level  $E_{tot} = E + E^c + X + X^c$ ) there is one stable steady state of the phosphorylated nuclear substrate,  $S^*$ , whereas for intermediate stimulus doses two stable steady states coexist (Figs. 2A-C). As the stimulus level changes (due to kinase production or degradation), the state of  $S^*$  may switch either to a highly or lowly phosphorylated (activity) steady state based on the system's memory: switching between states can occur in the form of a hysteresis loop (see black and red arrows in Fig. 2A).

Shuttling plays a pronounced role in modulating the number of discrete states of the nuclear substrate concentration  $S^*$  that can be realized: an increase of the shuttling rate constant causes the system to change either from a high to a low stable state (for  $k_{out,E}, k_{out,X}, k_{in,S}, k_{in,S^*}$ ) or *vice versa* (for  $k_{in,E}, k_{in,X}, k_{out,S}, k_{out,S^*}$ ), with an unstable steady state in between (Fig. 3A) and saddle node bifurcations. Depending on which rate constants are altered the resulting switches can be reversible (Fig. 3A,  $k_{out,E}, k_{in,X}$ ) or irreversible (Fig. 3A,  $k_{in,S^*}$ ). The response curves of the rate constants  $k_{in,E}, k_{in,S^*}, k_{out,X}, k_{out,S}$  can be tuned by altering *e.g.*, the total kinase levels, in order to alter the size of multistable regimes (Fig. 3B) or to turn reversible into irreversible switches. For example, if the shuttling rate constant  $k_{in,S^*}$  is small, then the nuclear  $S^*$  can exist in either a high or low state (bistable region); however, following an increase of the shuttling rate constant across a threshold, the system switches to a monostable low state and cannot switch back to the high state nor re-enter the bistable regime. Similarly the rate constants  $k_{out,S}, k_{in,E}$  provide irreversible switches favoring the high state. As the shuttling rate constants are controlled by a variety of other processes this endows spatially structured systems with a high level of flexibility and increased information-processing ability compared to spatially homogeneous systems: for example, any violation of the inequalities, Eqns. (6), may result in induction of multiple stable states.

## 1.2 MAPK two-site phosphorylation

Having established that species shuttling introduces multistability in a system that otherwise is monostable, we next explore the influence of shuttling in a system that can already exhibit multistability. Specifically, we consider nuclear localization in a two-site phosphorylation cycle (Fig. 4A), such as the layers of

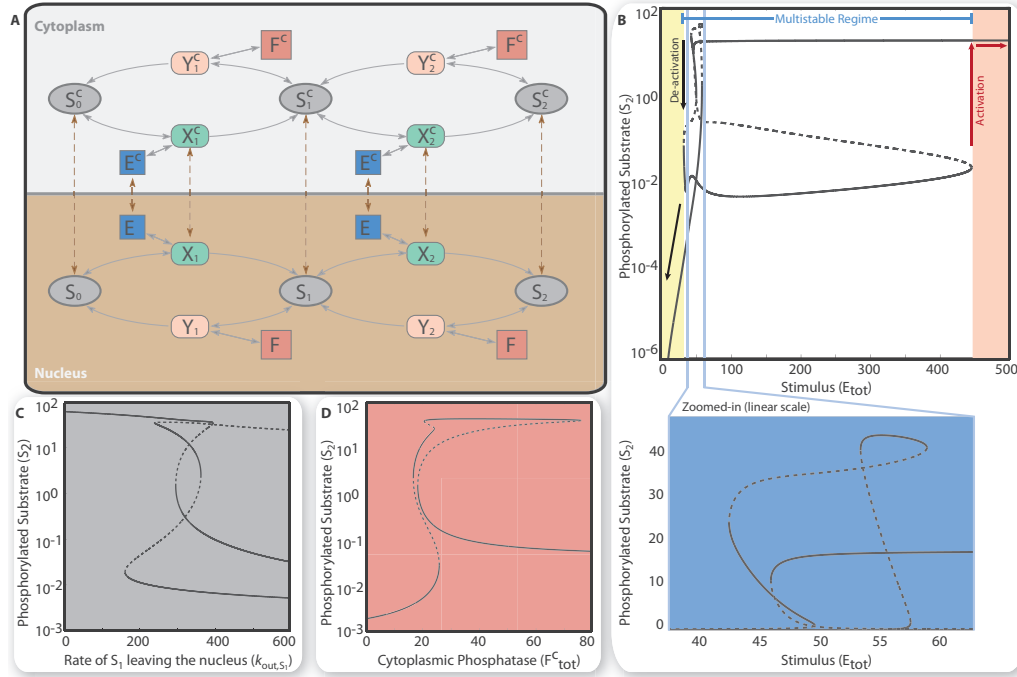


Figure 4: Two site phosphorylation localization model. Rate constants and total amounts provided in the Appendix. (A) Schematic of two-site phosphorylation/dephosphorylation in two compartments, cytoplasm and nucleus. (B) Steady state curve of phosphorylated nuclear substrate ( $S_2$ ) shows multistability and hysteresis as a function of stimulus (total kinase  $E_{tot}$ ). Stable states, solid lines; unstable states, dashed lines. Activation (phosphorylation) and deactivation (dephosphorylation) switches discontinuously from one stable branch to another at different stimulus thresholds, corresponding to the boundary values of the multistable regime (blue interval). Extreme values of stimulus restrict the system to monostability (log scale). Closer inspection reveals up to four stable states simultaneously (blue figure, zoomed, linear scale). (C, D) Steady state curve of phosphorylated nuclear substrate ( $S_2$ ) as a function of the rate constant of  $S_1$  shuttling out of the nucleus ( $k_{out,S_1}$ ) (gray) or as a function of the total cytoplasmic phosphatase ( $F_{tot}^C$ ) (coral).

canonical MAPK cascades, and its impact on the cell's ability to establish distinct stable states. Multistability, known to exist in these systems [23] with up to three stable states [24], has been discussed without reference to any of the spatial models of MAPK signaling [9, 12, 22, 25, 26]. Here, in order to differentiate between biochemical dependent and shuttling-dependent multistability, we consider biochemical parameter sets that preclude multistability in the absence of localization (see Appendix). Again spatial structure and shuttling between compartments can induce bistability; *e.g.*, fixing the shuttling species to be  $E$ ,  $X_1$ ,  $X_2$ ,  $S_0$ ,  $S_1$ ,  $S_2$ , bistability is introduced in the system (see Appendix). Provided that the rate constants in at least one of the cycles are in the range of multistability of the two-site phosphorylation cycle, we observe that shuttling creates up to 4 stable states and 3 unstable states (Fig. 4B). Steady state analysis on a choice of biologically plausible shuttling rates indicates that with shuttling the two-site phosphorylation cycle can undergo hysteresis effects with a large region of multistability ( $32 \leq E_{tot} \leq 445$ ), most of which is bistable. The doubly-phosphorylated substrate in the nucleus ( $S_2$ ) appears in a low/high monostable state for extremely low/high levels of kinase  $E_{tot}$  (red and black arrows in Fig. 4B).

The extended region of multistability with four stable states may provide an explanation for the versatility of MAPK signaling systems and their widespread use as relays in many signal transduction networks; it furthermore confers simultaneously both increased robustness and flexibility to the signal processing capabilities of the system compared to spatially homogeneous alternatives. As expected, the steady states of

the system can be regulated through *reversible switches* governed by shuttling parameters and other total amounts (Figs. 4C, D). But in some cases, stable states may be so close together to be virtually indistinguishable under some physiological conditions; the switching between 3 and 4 stable states in a small region (see zoomed box Fig. 4B) may be an example of this. This, too, can be modulated, however, by regulation of the shuttling process, or by adjusting total substrate abundances.

## 2 Discussion

Fidelity of information processing and the computational capacity, *i.e.*, the ability to map environmental states onto discernible internal states (in particular of proteins active in the nucleus), are thus profoundly affected by the spatial structure of eukaryotic cells. In a biological context, a high and stable state of nuclear substrate ( $S^*$ ) can marshal robust responses to environmental cues. To add further flexibility to such information processing the shuttling speed of a substrate may further depend on the nature of the stimulus; biological examples abound, and, for example, stimulated NIH 3T3 cells shuttle MAPK into the nucleus three times faster than starved cells [27]. By simultaneously controlling the stimulus dose and shuttling speed, a nuanced transition to reversible bistability permits hysteresis, and thus introduces the possibility for switching between low and high stable states (Fig. 3B).

Trafficking is therefore more intimately related to cellular computation than is typically acknowledged and differences between cell lines in the shuttling rate constants of different substrates — *e.g.*, in NIH 3T3 mouse cells, phospho-MAPK can accumulate in the nucleus [27]; whereas nuclear accumulation does not occur in PC12 cells [28] — may be hard-wired. Alternatively, the rich set of mechanisms affecting both phosphorylation (exemplary perhaps also for other post-translational modifications) and trafficking give cells the flexibility to change their dynamical regime, *e.g.*, from monostable to multistable, on the fly and in response to further environmental and physiological cues. The spatial/compartamental organization of cells thus drives crucial aspects of their information processing capacity; notably the number and robustness of states that can be stably represented is higher (or at least as high) for spatially structured systems compared to homogeneous systems [1]. This provides a further rationale for the evolution of cellular compartments [29] but also begs the question as to how bacteria and archaea can increase their computational capacities. Here, we believe, micro-environments generated by molecular crowding [30] confer some of the same advantages. Crowding, *e.g.*, around membrane associated histidine kinases of two-component signaling systems, can isolate signal transduction components spatially from one another, which would have similar (although likely weaker) impact on the computational *address space* as cellular compartment have in eukaryotes.

**Acknowledgments.** The authors gratefully acknowledge funding from The Leverhulme Trust. MPHS is a Royal Society Wolfson Research Merit Award holder. EF is supported by the fellowship “Beatriu de Pinós” from the Generalitat de Catalunya and the research project MTM2009-14163-C02-01 from Spain. CW is supported by the Danish Research Council and the Lundbeck Foundation, Denmark.

## A Appendix: Supporting information

In the Supporting Information we illustrate the claims made in the main text in more detail. We further expand on the heuristic methods that we have developed to determine if a system of biochemical reactions has the capacity for multiple steady states and to find conditions on the rate constants that ensure that multiple steady states cannot occur. In Section A.1 we give an overview of the methods employed. In Section A.2 we study a one-site phosphorylation cycle, which is monostationary, and show that shuttling species can introduce multistationarity. In Section A.3 we study the extended two-site phosphorylation cycle. Without compartmentalization the two-site modification cycle exhibits multistationarity for some

choices of rate constants but not all. We show that compartmentalization can introduce multistationarity even if the rate contents do not allow multistationarity in a two-site system without compartmentalization.

### A.1 Methods for the determination and preclusion of multistationarity

We derive conditions on the rate constants that ensure multistationarity cannot occur. Let

$$f = (f_1, \dots, f_n): \mathbb{R}^n \rightarrow \mathbb{R}^n$$

be a differentiable function. The Jacobian,  $J_x(f)$ , of  $f$  at a point  $x = (x_1, \dots, x_n)$  in  $\mathbb{R}^n$  is the  $n \times n$  matrix with entry  $(i, j)$  being  $\frac{\partial f_i}{\partial x_j}$ . If  $f$  is a polynomial function then all entries of the matrix  $J_x(f)$  are polynomials in  $x$  and consequently, the determinant of  $J_x(f)$  is a polynomial in  $x$  too. The Jacobian injectivity criterion states that if all components  $f_i$  have total degree at most two, and the determinant of the Jacobian does not vanish in a convex domain  $\Omega \subseteq \mathbb{R}^n$ , then  $f$  is an injective function in  $\Omega$  [18].

The positive steady states of a system of biochemical reactions are given as the positive solutions to a system of polynomial equations  $f_{\kappa,i}(x) = 0$ ,  $i = 1, \dots, n$ , where the coefficients of polynomials  $f_{\kappa,i}$  depend on the rate constants  $\kappa = \{k_r\}$  and  $k_r$  is the rate constant of reaction  $r$ . If the function  $f_\kappa = (f_{\kappa,1}, \dots, f_{\kappa,n})$  is injective over the positive real numbers  $\mathbb{R}_+^n$  then there can at most be one positive solution to  $f_\kappa(x) = (0, \dots, 0)$ , and consequently, multistationarity cannot occur. We will use the Jacobian injectivity criterion with  $\Omega = \mathbb{R}_+^n$  to determine if the function  $f_\kappa$  is injective.

In our case, the polynomials  $f_{\kappa,i}$  are either quadratic or linear, and hence the Jacobian injectivity criterion can be applied. The determinant of the Jacobian of  $f_\kappa$  is a polynomial in  $x$  with coefficients depending on the rate constants. Each term in the polynomial is of the form  $a(\kappa)x_1^{m_1} \cdots x_n^{m_n}$ , where  $a(\kappa)$  is a coefficient and  $m_j$  is 0, 1 or 2. If the coefficients of the determinant of the Jacobian are all positive or all negative for a specific choice of rate constants, then the determinant cannot vanish when  $x$  is positive. Hence, it follows from the Jacobian injectivity criterion that multiple positive steady states cannot occur. Importantly the coefficients  $a(\kappa)$  themselves are polynomials in the rate constants  $\kappa = \{k_r\}$ . Thus, we can study how the signs of the coefficients vary when the rate constants vary. Our focus is on analyzing the coefficients in order to understand what combinations of rate constants make them all positive or all negative.

The role of the Jacobian injectivity criterion is to preclude multistationarity. However, failure of the Jacobian injectivity criterion is not sufficient to conclude that multistationarity occurs. To investigate whether multistationarity occurs when the Jacobian injectivity criterion fails, we make use of the algorithms implemented in the chemical reaction network theory (CRNT) toolbox [20]. For some systems modeled with mass-action kinetics (as is the case here), the toolbox can conclusively determine if multistationarity can occur or not. If the system admits multiple steady states, the toolbox outputs a unique set of rate constants for which there exists a pair of positive steady states (fulfilling the conservation laws with the same total amounts). However, the rate constants that the toolbox outputs cannot be constrained or controlled in any way. That is to say, we cannot ask the toolbox to restrict the search to certain regions that are considered biologically realistic. This limits substantially the use of the algorithms of the toolbox. Nevertheless, the output rate constants serve here as a starting point for further investigation and manipulation.

In this work, a steady state is considered stable if it is asymptotically stable, that is, if the real part of the eigenvalues of the Jacobian of the system at the steady state are all negative. Asymptotic stability ensures that if the initial state of the system is sufficiently close to the steady state then it will eventually be attracted towards the steady state.



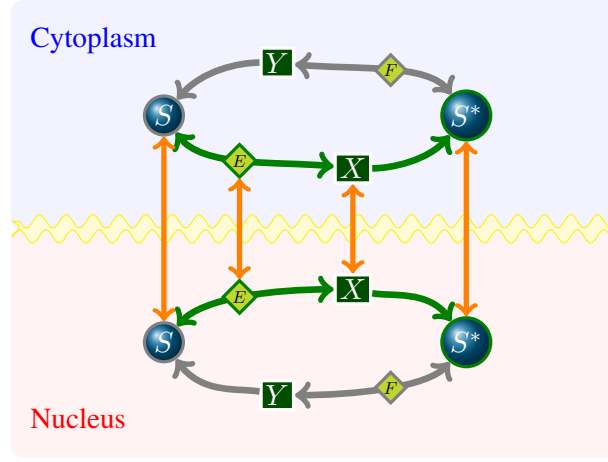


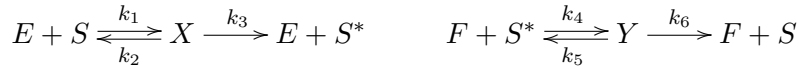
Figure 5: Shuttling of a one-site phosphorylation cycle between the nucleus and the cytoplasm.

## A.2 Shuttling in a one-site phosphorylation cycle

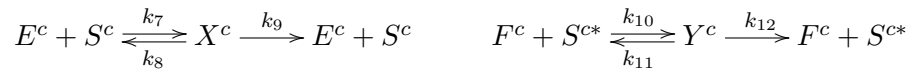
**Reactions and rate constants.** We consider a one-site phosphorylation cycle with species  $S, S^*$  (the unphosphorylated and phosphorylated substrates),  $E$  (kinase),  $F$  (phosphatase), and  $X, Y$  (intermediate complexes). Phosphorylation and dephosphorylation are assumed to follow a Michaelis-Menten mechanism (see below and main text). This motif cannot admit multiple steady states and is monostable [16].

To study the effect of compartmentalization we assume that the species  $S, S^*, E, X$  can shuttle between the cytoplasm and the nucleus (see Figure 5). We let  $Z^c$  denote the species  $Z$  in the cytoplasm. Then, we have the following reactions:

- Reactions in the nucleus:



- Reactions in the cytoplasm:



- Shuttling reactions:



To ease the notation, we have changed the notation of the reaction constants  $k_r$  in the main text and simply labeled them with consecutive numbers  $k_1, \dots, k_{20}$ . The correspondence between the two notations is shown below:

Here	$k_1$	$k_2$	$k_3$	$k_4$	$k_5$	$k_6$	$k_7$	$k_8$	$k_9$	$k_{10}$
Main text	$k_{\text{on},E}$	$k_{\text{off},E}$	$k_{\text{cat},E}$	$k_{\text{on},F}$	$k_{\text{off},F}$	$k_{\text{cat},F}$	$k_{\text{on},E}^c$	$k_{\text{off},E}^c$	$k_{\text{cat},E}^c$	$k_{\text{on},F}^c$
Here	$k_{11}$	$k_{12}$	$k_{13}$	$k_{14}$	$k_{15}$	$k_{16}$	$k_{17}$	$k_{18}$	$k_{19}$	$k_{20}$
Main text	$k_{\text{off},F}^c$	$k_{\text{cat},F}^c$	$k_{\text{out},E}$	$k_{\text{out},X}$	$k_{\text{out},S}$	$k_{\text{out},S^*}$	$k_{\text{in},E}$	$k_{\text{in},X}$	$k_{\text{in},S}$	$k_{\text{in},S^*}$

**Mass-action system of ordinary differential equations.** We order the set of species in the following way:

$$(x_1, x_2, x_3, x_4, x_5, x_6) = (E, X, S, S^*, F, Y), \quad (x_7, x_8, x_9, x_{10}, x_{11}, x_{12}) = (E^c, X^c, S^c, S^{c*}, F^c, Y^c).$$

By assuming the law of mass-action, the dynamics of this reaction network is modeled by the following system of ordinary differential equations (reference to time  $t$  is omitted,  $x_i = x_i(t)$ ):

$$\begin{aligned}
\dot{x}_1 &= -k_{13}x_1 + k_2x_2 + k_3x_2 - k_1x_1x_3 + k_{17}x_7, \\
\dot{x}_2 &= -k_2x_2 - k_3x_2 - k_{14}x_2 + k_1x_1x_3 + k_{18}x_8, \\
\dot{x}_3 &= k_2x_2 - k_{15}x_3 - k_1x_1x_3 + k_6x_6 + k_{19}x_9, \\
\dot{x}_4 &= k_3x_2 - k_{16}x_4 - k_4x_4x_5 + k_5x_6 + k_{20}x_{10}, \\
\dot{x}_5 &= -k_4x_4x_5 + k_5x_6 + k_6x_6, \\
\dot{x}_6 &= k_4x_4x_5 - k_5x_6 - k_6x_6, \\
\dot{x}_7 &= k_{13}x_1 - k_{17}x_7 + k_8x_8 + k_9x_8 - k_7x_7x_9, \\
\dot{x}_8 &= k_{14}x_2 - k_8x_8 - k_9x_8 - k_{18}x_8 + k_7x_7x_9, \\
\dot{x}_9 &= k_{15}x_3 + k_8x_8 - k_{19}x_9 - k_7x_7x_9 + k_{12}x_{12}, \\
\dot{x}_{10} &= k_{16}x_4 + k_9x_8 - k_{20}x_{10} - k_{10}x_{10}x_{11} + k_{11}x_{12}, \\
\dot{x}_{11} &= -k_{10}x_{10}x_{11} + k_{11}x_{12} + k_{12}x_{12}, \\
\dot{x}_{12} &= k_{10}x_{10}x_{11} - k_{11}x_{12} - k_{12}x_{12}.
\end{aligned} \tag{7}$$

This dynamical system has four conservation laws, accounting for the fact that the amounts of enzymes and substrate are conserved:

$$\begin{aligned}
0 &= \dot{x}_1 + \dot{x}_2 + \dot{x}_7 + \dot{x}_8, \\
0 &= \dot{x}_5 + \dot{x}_6, \\
0 &= \dot{x}_2 + \dot{x}_3 + \dot{x}_4 + \dot{x}_6 + \dot{x}_8 + \dot{x}_9 + \dot{x}_{10} + \dot{x}_{12}, \\
0 &= \dot{x}_{11} + \dot{x}_{12}.
\end{aligned} \tag{8}$$

These conservation laws can be verified but adding the corresponding equations in (7). Since the model does not incorporate shuttling of the phosphatase, the amount of phosphatase is conserved separately in each compartment.

Let  $S_{tot}$  denote the total amount of substrate, and  $E_{tot}, F_{tot}, F_{tot}^c$  denote the total amounts of kinase and phosphatase in the system, respectively. The differential equations in (8) lead to the following equations that are fulfilled at any time:

$$\begin{aligned}
E_{tot} &= x_1 + x_2 + x_7 + x_8 \\
F_{tot} &= x_5 + x_6 \\
S_{tot} &= x_2 + x_3 + x_4 + x_6 + x_8 + x_9 + x_{10} + x_{12} \\
F_{tot}^c &= x_{11} + x_{12}.
\end{aligned} \tag{9}$$

The steady states of the system are obtained by setting all derivatives  $\dot{x}_i$  to zero. The system has the *capacity for multiple steady states* if there exist rate constants  $k_1, \dots, k_{20}$  and positive total amounts  $S_{tot}, E_{tot}, F_{tot}, F_{tot}^c$  such that the equations  $\dot{x}_i = 0$  together with (9) have more than one positive solution. Therefore, for fixed reaction rates and total amounts, determination of multistationarity implies solving a system of polynomial equations in 12 indeterminates (variables). The equations corresponding to the conservation laws are linear, while those corresponding to setting the derivatives to zero are quadratic (that is, they have terms of total degree 1 and 2).

**Rate constants and total amounts for multistationarity (for Figs. 2, 3 in the main text).** The CRNT toolbox provides a unique set of rate constants for which the system admits multiple positive steady states

$$\begin{aligned} k_1 &= 11.679195 & k_2 &= 144.94137 & k_3 &= 91.527059 & k_4 &= 207.26904 & k_5 &= 22.115015, \\ k_6 &= 309.97808, & k_7 &= 49.545796, & k_8 &= 8.8750284, & k_9 &= 262.90818, & k_{10} &= 356.03934, \\ k_{11} &= 1.8978202, & k_{12} &= 44.457164, & k_{13} &= 1.0903408, & k_{14} &= 305.42214, & k_{15} &= 47.547732, \\ k_{16} &= 41.866754, & k_{17} &= 86.473107, & k_{18} &= 215.67801, & k_{19} &= 1, & k_{20} &= 165.98446. \end{aligned}$$

For this set of rate constants, two steady states are provided with total amounts:

$$E_{tot} = 20.7066814, \quad S_{tot} = 35.21053215, \quad F_{tot} = 3.84921092, \quad F_{tot}^c = 11.0903086.$$

We aim to exemplify multistationarity with rate constants that are more biologically reasonable and of the order of experimentally determined values [9, 11]. To this end, we have manually investigated the effect of changing a specific rate or a total amount with respect to the emergence of multistationarity. We guide the proposed changes by the structure of the steady-state equations. This procedure has allowed us to tune the rate constants and total amounts to reasonable values without losing multistationarity. Specifically, we settled for the rates (used to create Figures 2 and 3 in the main text):

$$\begin{aligned} k_1 &= 0.049 & k_2 &= 0.009 & k_3 &= 0.262 & k_4 &= 0.356 & k_5 &= 0.002 & k_6 &= 0.044 & k_7 &= 0.011 \\ k_8 &= 0.144 & k_9 &= 0.091 & k_{10} &= 0.207 & k_{11} &= 0.022 & k_{12} &= 0.309 & k_{13} &= 0.16 & k_{14} &= 0.14 \\ k_{15} &= 0.001 & k_{16} &= 0.166 & k_{17} &= 0.0006 & k_{18} &= 0.33 & k_{19} &= 0.047 & k_{20} &= 0.041, \end{aligned}$$

and the total amounts  $\{E_{tot}, S_{tot}, F_{tot}, F_{tot}^c\} = \{22, 35, 11, 3\}$ . With these parameters, there are three steady states, of which two are stable. Specifically, the steady states are approximately:

$$\begin{aligned} SS_1 &= (0.676, 2.357, 16.33, 1.261, 1.023, 9.977, 17.671, 1.296, 2.068, 0.751, 2.041, 0.959) \\ SS_2 &= (0.183, 0.965, 27.220, 0.126, 5.623, 5.377, 20.391, 0.461, 0.559, 0.107, 2.812, 0.188) \\ SS_3 &= (1.062, 2.87, 11.847, 2.145, 0.625, 10.375, 16.371, 1.701, 3.109, 1.503, 1.546, 1.454). \end{aligned}$$

The steady state  $SS_1$  is unstable and has only one eigenvalue with positive real part.

**Conditions for monostationarity (Eqns (6) in the main text).** Not all choices of rate constants and total amounts have the capacity for multistationarity. We show here that there is a set of *necessary* conditions for the existence of multistationarity that depends exclusively on the shuttling rates. To see this, we apply the Jacobian injectivity criterion to a function that in part consists of the right hand sides of the conservation laws (7).

Specifically, we consider the polynomial function  $f_\kappa: \mathbb{R}^{12} \rightarrow \mathbb{R}^{12}$  given by the right-hand side of the four conservation equations (9) and the equations in (7) for all  $\dot{x}_i$  except for  $\dot{x}_1, \dot{x}_2, \dot{x}_5$  and  $\dot{x}_{11}$ . The latter equations are redundant and can be obtained from the conserved equations in (8). The 12 components of the function  $f_\kappa = (f_{\kappa,1}, \dots, f_{\kappa,12})$  are

$$\begin{aligned} f_{\kappa,1} &= x_1 + x_2 + x_7 + x_{11}, \\ f_{\kappa,2} &= x_2 + x_3 + x_4 + x_6 + x_8 + x_9 + x_{10} + x_{12}, \\ f_{\kappa,3} &= x_5 + x_6, \\ f_{\kappa,4} &= x_{11} + x_{12}, \\ f_{\kappa,5} &= k_2 x_2 - k_{15} x_3 - k_1 x_1 x_3 + k_6 x_6 + k_{19} x_9, \\ f_{\kappa,6} &= k_3 x_2 - k_{16} x_4 - k_4 x_4 x_5 + k_5 x_6 + k_{20} x_{10}, \\ f_{\kappa,7} &= k_4 x_4 x_5 - k_5 x_6 - k_6 x_6, \\ f_{\kappa,8} &= k_{13} x_1 - k_{17} x_7 + k_8 x_8 + k_9 x_8 - k_7 x_7 x_9, \\ f_{\kappa,9} &= k_{14} x_2 - k_8 x_8 - k_9 x_8 - k_{18} x_8 + k_7 x_7 x_9, \\ f_{\kappa,10} &= k_{15} x_3 + k_8 x_8 - k_{19} x_9 - k_7 x_7 x_9 + k_{12} x_{12}, \\ f_{\kappa,11} &= k_{16} x_4 + k_9 x_8 - k_{20} x_{10} - k_{10} x_{10} x_{11} + k_{11} x_{12}, \\ f_{\kappa,12} &= k_{10} x_{10} x_{11} - k_{11} x_{12} - k_{12} x_{12}. \end{aligned}$$

If this function is injective over the real positive numbers  $\mathbb{R}_+^n$ , then multiple positive steady states with the same total amounts cannot occur. As described in Section A.1, we use the Jacobian injectivity criterion to investigate conditions on the rate constants for which the function is injective. Since  $f_\kappa$  is quadratic, the criterion applies. The determinant of the Jacobian of  $f_\kappa$  can be computed using any software that enables algebraic (symbolic) computations, like Mathematica or Maple. We compute the determinant and extract the coefficients. These coefficients are polynomials in the rate constants and most of them contain only positive summands. Therefore, we search for the coefficients that have negative summands. After appropriate factorization and simplification, we conclude that the coefficients are all positive if and only if the following expressions are positive:

$$\begin{aligned}
C_1 &= k_9 k_{14} + k_9 k_{17} + k_3(k_{18} - k_{17}) = k_9 k_{14} + (k_9 - k_3)k_{17} + k_3 k_{18}, \\
C_2 &= k_3 k_{12}(k_{15} - k_{16})(k_{18} - k_{17}) + k_3 k_{15} k_{16}(k_{18} - k_{17}) + k_{12} k_{15} k_{16} k_{18} + k_9 k_{14} k_{15} k_{16} \\
&\quad + k_{12} k_{14} k_{15} k_{16} + k_{12} k_{14} k_{16} k_{17} + k_9 k_{15} k_{16} k_{17} + k_{12} k_{16} k_{17} k_{18}, \\
C_3 &= k_3 k_{12} k_{15}(k_{18} - k_{17}) + k_6 k_9 k_{14} k_{15} + k_6 k_{12} k_{14} k_{15} + k_6 k_{12} k_{14} k_{17} + k_6 k_9 k_{15} k_{17} \\
&\quad + k_6 k_{12} k_{15} k_{18} + k_6 k_{12} k_{17} k_{18}, \\
C_4 &= k_3 k_{15}(k_{18} - k_{17})k_{20} + k_6 k_9 k_{14} k_{15} + k_6 k_9 k_{15} k_{17} + k_6 k_9 k_{14} k_{20} + k_6 k_{14} k_{15} k_{20} \\
&\quad + k_9 k_{14} k_{15} k_{20} + k_6 k_9 k_{17} k_{20} + k_6 k_{14} k_{17} k_{20} + k_9 k_{15} k_{17} k_{20} + k_6 k_{15} k_{18} k_{20} + k_6 k_{17} k_{18} k_{20}, \\
C_5 &= k_3 k_{13} + k_9(k_{14} - k_{13}) + k_3 k_{18} = (k_3 - k_9)k_{13} + k_9 k_{14} + k_3 k_{18}, \\
C_6 &= k_6 k_9(k_{14} - k_{13})k_{19} + k_6 k_{12} k_{13} k_{14} + k_6 k_{12} k_{13} k_{18} + k_3 k_{12} k_{13} k_{19} + k_6 k_{12} k_{14} k_{19} \\
&\quad + k_3 k_{12} k_{18} k_{19} + k_6 k_{12} k_{18} k_{19}, \\
C_7 &= k_9(k_{14} - k_{13})k_{16} k_{19} + k_3 k_{12} k_{13} k_{16} + k_{12} k_{13} k_{14} k_{16} + k_3 k_{12} k_{16} k_{18} + k_{12} k_{13} k_{16} k_{18} \\
&\quad + k_3 k_{12} k_{13} k_{19} + k_3 k_{13} k_{16} k_{19} + k_{12} k_{14} k_{16} k_{19} + k_3 k_{12} k_{18} k_{19} + k_3 k_{16} k_{18} k_{19} + k_{12} k_{16} k_{18} k_{19}, \\
C_8 &= k_6 k_9(k_{14} - k_{13})(k_{19} - k_{20}) + k_9(k_{14} - k_{13})k_{19} k_{20} + k_6 k_{13} k_{14} k_{20} + k_6 k_{13} k_{18} k_{20} \\
&\quad + k_3 k_{13} k_{19} k_{20} + k_6 k_{14} k_{19} k_{20} + k_3 k_{18} k_{19} k_{20} + k_6 k_{18} k_{19} k_{20}.
\end{aligned}$$

Observe that these expressions *only* involve the 8 shuttling rates and  $k_3, k_6, k_9, k_{12}$ . Instances for which the coefficients  $C_1, \dots, C_8$  are negative exist. If

$$k_{20} \leq k_{19}, \quad k_{18} \geq k_{17}, \quad k_{16} \leq k_{15}, \quad k_{14} \geq k_{13}, \quad (10)$$

then  $C_i > 0$  for all  $i$  and hence multistationarity cannot occur for any choice of total amounts (these inequalities correspond to Eqns. (6) in the main text). However, there is no guarantee that when these conditions fail, the system admits multiple steady states for some total amounts. Figure 5 above is reproduced as Figure 6 with the shuttling rate constants indicated.

We assume now that the dissociation constants are the same in the two compartments (the nucleus and the cytoplasm), that is, we assume that  $k_3 = k_9$  and  $k_6 = k_{12}$ . In this case  $C_i > 0$  for all  $i \neq 2, 8$  and all shuttling rate constants. Therefore, two conditions suffice to guarantee monostationarity, namely:

$$\begin{aligned}
\tilde{C}_2 &= k_9 k_{12}(k_{15} - k_{16})(k_{18} - k_{17}) + k_9 k_{14} k_{15} k_{16} + k_{12} k_{14} k_{15} k_{16} \\
&\quad + k_{12} k_{14} k_{16} k_{17} + k_9 k_{15} k_{16} k_{18} + k_{12} k_{15} k_{16} k_{18} + k_{12} k_{16} k_{17} k_{18} > 0, \\
\tilde{C}_8 &= k_9 k_{12}(k_{14} - k_{13})(k_{19} - k_{20}) + k_{12} k_{13} k_{14} k_{20} + k_{12} k_{13} k_{18} k_{20} \\
&\quad + k_9 k_{14} k_{19} k_{20} + k_{12} k_{14} k_{19} k_{20} + k_9 k_{18} k_{19} k_{20} + k_{12} k_{18} k_{19} k_{20} > 0.
\end{aligned}$$

The first corresponds to  $C_2$  and the second to  $C_8$ . By inspection of these two expressions, we conclude that multistationarity cannot occur in any of the following cases:

- (i)  $k_{20} \leq k_{19}, \quad k_{18} \geq k_{17}, \quad k_{16} \leq k_{15}, \quad k_{14} \geq k_{13},$
- (ii)  $k_{20} \geq k_{19}, \quad k_{18} \geq k_{17}, \quad k_{16} \leq k_{15}, \quad k_{14} \leq k_{13},$
- (iii)  $k_{20} \leq k_{19}, \quad k_{18} \leq k_{17}, \quad k_{16} \geq k_{15}, \quad k_{14} \geq k_{13},$
- (iv)  $k_{20} \geq k_{19}, \quad k_{18} \leq k_{17}, \quad k_{16} \geq k_{15}, \quad k_{14} \leq k_{13}.$

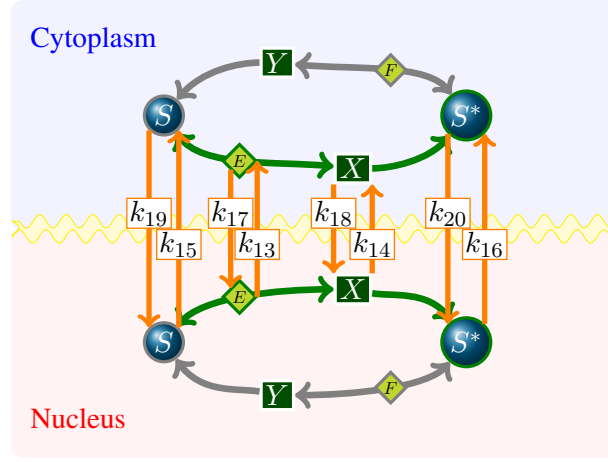


Figure 6: Shuttling rates for the one-site phosphorylation cycle

Note that these *only* involve the rate constants for the shuttling reactions. If the dissociation rate constants are not exactly the same in the cytoplasm and in the nucleus, but very similar, then the conditions above are still sufficient.

We see that the rate constants go in pairs: the shuttling rate constants of  $S$  relate to those of  $S^*$ , and the shuttling rate constants of  $E$  to those of  $X$ . In particular, the following conditions are necessary for multistationarity:

- (1) If  $X$  shuttles into the nucleus slower than  $E$  then  $S$  shuttles into the cytoplasm slower than  $S^*$  and vice versa.
- (2) If  $X$  shuttles into the cytoplasm slower than  $E$  then  $S$  shuttles into the nucleus slower than  $S^*$  and vice versa.

Sets of rate constants for which  $I_1 < 0$  can for instance be obtained by letting the product  $k_9k_{16}$  be large and the remaining products be small such that  $k_{14}k_{15} + k_{12}k_{17} - k_{12}k_{18} + k_{15}k_{18} < 0$  is satisfied.

#	No multistationarity	Multistationarity
1	All	None
2	$\{S, S^*\} \{E, Y\} \{F, X\} \{S^*, E\}$ $\{S, F\} \{S, X\} \{S^*, Y\} \{E, X\}$ $\{F, Y\} \{S, E\} \{S^*, F\}$	$\{E, F\} \{X, Y\} \{S^*, X\} \{S, Y\}$
3	$\{X, E, F\} \{Y, E, F\} \{X, Y, E\}$ $\{X, Y, F\} \{S, F, X\} \{S^*, E, Y\}$ $\{S, E, F\} \{S^*, F, E\}$	$\{S, E, X\} \{S^*, F, Y\} \{S, E, Y\} \{S^*, E, X\}$ $\{S^*, F, X\} \{S, E, S^*\} \{S^*, F, S\} \{S, S^*, X\}$ $\{S, X, Y\} \{S^*, Y, X\} \{S, F, Y\} \{S, S^*, Y\}$
4	$\{Y, X, E, F\}$	$\{S, S^*, X, F\} \{S, S^*, Y, E\} \{S, E, X, Y\} \{S^*, F, X, Y\}$ $\{S, F, X, Y\} \{S^*, E, X, Y\} \{S, S^*, X, Y\} \{S, S^*, E, F\}$ $\{S, E, F, X\} \{S^*, E, F, Y\} \{S, E, F, Y\}$ $\{S^*, E, F, X\} \{S, S^*, X, E\} \{S, S^*, Y, F\}$
5, 6	None	All

Table 1: One-site phosphorylation system. For all possible sets of shuttling species it is indicated if the system has the capacity for multiple steady states or not.

**Sets of shuttling species and multistationarity.** We have shown that if the species  $E, X, S, S^*$  shuttle between compartments, multistationarity is created. We next investigate what the sets of shuttling species

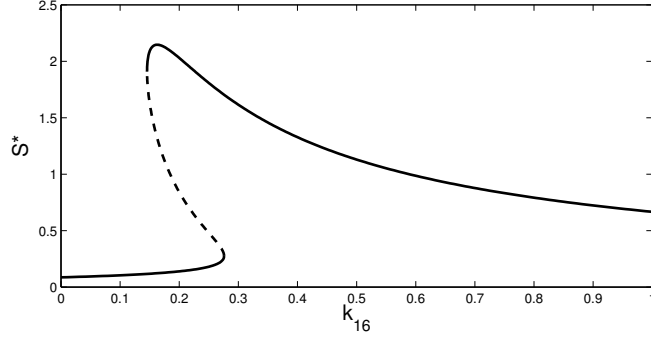


Figure 7: The response  $S^*$  plotted against the rate constant  $k_{16}$ , at baseline total amounts.

that provide multistationarity are. The results are summarized in Table 1. We use a systematic way to classify each motif: First, we check if the system fulfills the Jacobian injectivity criterion for all rate constants. If the coefficients of the polynomial in  $x$  given by the determinant of the Jacobian (as above) are all positive, then the system cannot exhibit multistationarity for any set of total amounts (see also [21]). If the criterion fails then we use the CRNT toolbox.

We have obtained that if only one species shuttles then multistationarity cannot occur. That is, at least two species, e.g.  $\{S^*, X\}$  or  $\{S, Y\}$ , are required to create multistationarity in the one-site phosphorylation cycle for certain total amounts and rate constants. The addition of shuttling species maintains multistationarity.

**Effects of varying the shuttling rates.** We analyze the steady-state response of  $S^*$  in the nucleus as the shuttling rate constants and total amounts change in the system.

The following table summarizes the type of saddle-node bifurcation curves obtained as shuttling rate constants of molecular species are varied.

Rate constant	Rate-response curve
$k_{13}, k_{14}, k_{19}, k_{20}$	For large rate constant, only a low stable steady state is obtained
$k_{15}, k_{17}, k_{18}$	For a small rate constant, only a high stable steady state is obtained
$k_{16}$	Similar to the previous case, but the high branch decreases (Fig. 7).

By varying a total amount and shuttling rate constant simultaneously, the system may undergo irreversible switches. This occurs with respect to shuttling rate constants  $k_{14}, k_{15}, k_{17}$ , and  $k_{20}$ . Specifically, for shuttling parameters,  $k_{15}$  and  $k_{17}$ , the irreversible switch is obtained by either increasing  $F_{tot}$  or decreasing  $E_{tot}, S_{tot}$  or  $F_{tot}^c$ . As the value of the shuttling rate constant increases, the response curve switches from a low to a high steady state, favoring accumulation in the nucleus. Conversely, increasing the value of shuttling parameters  $k_{14}$  and  $k_{20}$  induces an irreversible switch from the high to low steady-state by either decreasing  $F_{tot}$  or increasing  $E_{tot}, S_{tot}$ . As highlighted in the main text (see Figure 3), the  $k_{20}$  bifurcation is irreversible at baseline parameter values.

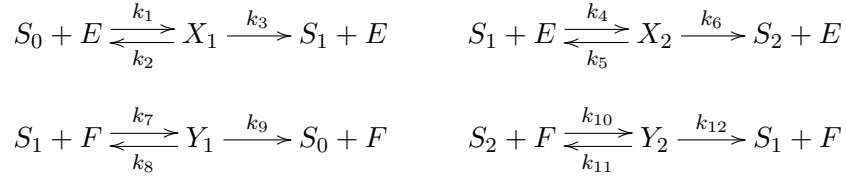
### A.3 Shuttling in a two-site phosphorylation cycle

In eukaryotes, most protein phosphorylation events take place in more than one site. It is well known that multisite phosphorylation can cause multistationarity by itself [8, 23]. However, multistationarity does not occur for all choices of rate constants.

We next investigate the effect of adding species compartmentalization in a two-site (sequential) phosphorylation system. We first determine rate constants for which the two-site system cannot exhibit mul-

tistationarity. Then, we add species shuttling and determine shuttling rate constants that induce multistationarity.

**Conditions for monostationarity in a two-site phosphorylation cycle.** We consider a two-site phosphorylation cycle in which modifications take place sequentially. The reactions describing the system are:



The set of species is ordered such that

$$(x_1, \dots, x_9) = (E, X_1, S_0, S_1, F, Y_1, S_2, X_2, Y_2).$$

Assuming mass-action kinetics, then the differential equations describing the dynamics of the species concentrations are:

$$\begin{aligned} \dot{x}_1 &= k_2x_2 + k_3x_2 - k_1x_1x_3 - k_4x_1x_4 + k_5x_8 + k_6x_8, \\ \dot{x}_2 &= -k_2x_2 - k_3x_2 + k_1x_1x_3, \\ \dot{x}_3 &= k_2x_2 - k_1x_1x_3 + k_9x_6, \\ \dot{x}_4 &= k_3x_2 - k_4x_1x_4 - k_7x_4x_5 + k_8x_6 + k_5x_8 + k_{12}x_9, \\ \dot{x}_5 &= -k_7x_4x_5 + k_8x_6 + k_9x_6 - k_{10}x_5x_7 + k_{11}x_9 + k_{12}x_9, \\ \dot{x}_6 &= k_7x_4x_5 - k_8x_6 - k_9x_6, \\ \dot{x}_7 &= -k_{10}x_5x_7 + k_6x_8 + k_{11}x_9, \\ \dot{x}_8 &= k_4x_1x_4 - k_5x_8 - k_6x_8, \\ \dot{x}_9 &= k_{10}x_5x_7 - k_{11}x_9 - k_{12}x_9. \end{aligned}$$

This system has the following conserved amounts:

$$E_{tot} = x_1 + x_2 + x_8, \quad F_{tot} = x_5 + x_6 + x_9, \quad S_{tot} = x_2 + x_3 + x_4 + x_6 + x_7 + x_8 + x_9.$$

The steady-state equations are given by  $\dot{x}_i = 0$ . Because of the constraints given by the conservation laws, the equations  $\dot{x}_1 = 0$ ,  $\dot{x}_2 = 0$  and  $\dot{x}_5 = 0$  are redundant and can be removed.

We proceed as above to determine rate constants for which the system cannot have multiple steady states. That is, we apply the Jacobian injectivity criterion. We consider the function  $f_\kappa: \mathbb{R}^9 \rightarrow \mathbb{R}^9$  given by the three equations coming from the conservation laws and the 6 remaining steady-state equations:

$$\begin{aligned} f_{\kappa,1}(x) &= x_1 + x_2 + x_8, \\ f_{\kappa,2}(x) &= x_2 + x_3 + x_4 + x_6 + x_7 + x_8 + x_9, \\ f_{\kappa,3}(x) &= x_5 + x_6 + x_9, \\ f_{\kappa,4}(x) &= k_2x_2 - k_1x_1x_3 + k_9x_6, \\ f_{\kappa,5}(x) &= k_3x_2 - k_4x_1x_4 - k_7x_4x_5 + k_8x_6 + k_5x_8 + k_{12}x_9, \\ f_{\kappa,6}(x) &= k_7x_4x_5 - k_8x_6 - k_9x_6, \\ f_{\kappa,7}(x) &= -k_{10}x_5x_7 + k_6x_8 + k_{11}x_9, \\ f_{\kappa,8}(x) &= k_4x_1x_4 - k_5x_8 - k_6x_8, \\ f_{\kappa,9}(x) &= k_{10}x_5x_7 - k_{11}x_9 - k_{12}x_9. \end{aligned}$$

If this function is injective over the positive real numbers then multiple positive steady states cannot occur with the same total amounts in the conservation laws. Next, we compute the determinant of the Jacobian of  $f_\kappa$ . As a polynomial in  $x$ , the only coefficients (which depend on the rate constants  $k_i$ ) of the determinant that are not sums of positive terms are:

$$\begin{aligned} C_1 &= -k_2k_4k_6k_7k_9k_{10} - k_3k_4k_6k_7k_9k_{10} - k_1k_4k_6k_7k_9k_{11} - k_1k_4k_6k_7k_9k_{12} \\ &\quad + k_1k_3k_5k_7k_{10}k_{12} + k_1k_3k_6k_7k_{10}k_{12} + k_1k_3k_4k_8k_{10}k_{12} + k_1k_3k_4k_9k_{10}k_{12} \\ C_2 &= -k_1k_4k_7k_{10}(k_6k_9 - k_3k_{12}). \end{aligned}$$

If a choice of rate constants fulfills  $C_1, C_2 > 0$ , then the system cannot have multiple positive steady states for any total amounts. The coefficient  $C_1$  can be rewritten as

$$C_1 = -k_6k_9k_4k_7(k_2k_{10} + k_3k_{10} + k_1k_{11} + k_1k_{12}) + k_3k_{12}k_1k_{10}(k_5k_7 + k_6k_7 + k_4k_8 + k_4k_9).$$

For  $C_2 > 0$  we require

$$k_3/k_6 > k_9/k_{12}.$$

If this inequality is fulfilled then  $C_1 > 0$  if also

$$k_4k_7(k_2k_{10} + k_3k_{10} + k_1k_{11} + k_1k_{12}) < k_1k_{10}(k_5k_7 + k_6k_7 + k_4k_8 + k_4k_9).$$

This inequality can be rewritten as

$$\frac{k_2 + k_3}{k_1} + \frac{k_{11} + k_{12}}{k_{10}} < \frac{k_5 + k_6}{k_4} + \frac{k_8 + k_9}{k_7}.$$

Let

$$\alpha_1 = \frac{k_5 + k_6}{k_4} - \frac{k_2 + k_3}{k_1}, \quad \alpha_2 = \frac{k_8 + k_9}{k_7} - \frac{k_{11} + k_{12}}{k_{10}}, \quad \alpha_3 = \frac{k_3}{k_6} - \frac{k_9}{k_{12}}.$$

If

$$\alpha_1, \alpha_2, \alpha_3 > 0, \tag{11}$$

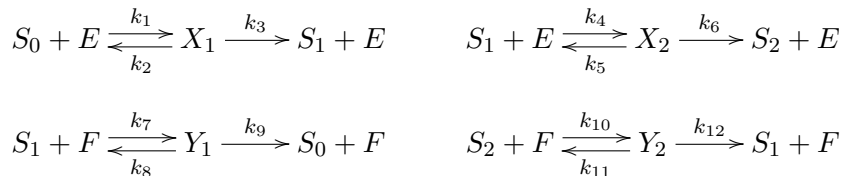
then the two-site phosphorylation system cannot have multiple positive steady states no matter the values of the total amounts. That is, a sufficient condition for the preclusion of multistationarity is obtained.

Observe that  $\alpha_1$  and  $\alpha_2$  imply an inequality between the Michaelis-Menten constants of the kinase and the phosphatase in each phosphorylation site. Namely, the Michaelis-Menten constant of  $E$  for the second site is larger than that for the first phosphorylation site, and the Michaelis-Menten constant of  $F$  for the first site is larger than that for the second site.

Negation of this condition is a priori not sufficient to guarantee multistationarity. However, if  $\alpha_3 < 0$ , then there exist total amounts for which the motif exhibits multistationarity [31].

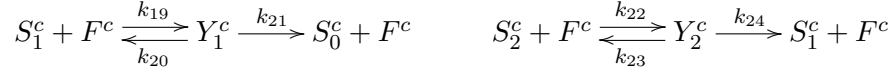
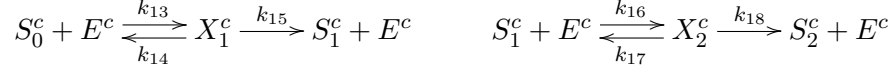
**Mass-action system of ordinary differential equations for the two-site shuttling.** Consider now two copies of a two-site phosphorylation cycle as above and let  $S_0, S_1, S_2, X_1, X_2, E$  shuttle between the nucleus and the cytoplasm. The reactions describing the system are:

- Reactions in the nucleus:

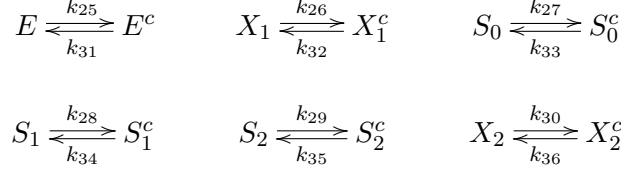




- Reactions in the cytoplasm:



- Shuttling reactions:



The species are ordered as:

$$(x_1, \dots, x_9) = (E, X_1, S_0, S_1, F, Y_1, S_2, X_2, Y_2)$$

$$(x_{10}, \dots, x_{18}) = (E^c, X_1^c, S_0^c, S_1^c, F^c, Y_1^c, S_2^c, X_2^c, Y_2^c).$$

Assuming mass-action kinetics, the system of differential equations describing the dynamics of the concentrations of the species is:

$$\begin{aligned} \dot{x}_1 &= k_2x_2 + k_3x_2 - k_1x_1x_3 - k_4x_1x_4 + k_5x_8 + k_6x_8 - k_{25}x_1 + k_{31}x_{10}, \\ \dot{x}_2 &= -k_2x_2 - k_3x_2 + k_1x_1x_3 - k_{26}x_2 + k_{32}x_{11}, \\ \dot{x}_3 &= k_2x_2 - k_1x_1x_3 + k_9x_6 - k_{27}x_3 + k_{33}x_{12}, \\ \dot{x}_4 &= k_3x_2 - k_4x_1x_4 - k_7x_4x_5 + k_8x_6 + k_5x_8 + k_{12}x_9 - k_{28}x_4 + k_{34}x_{13}, \\ \dot{x}_5 &= -k_7x_4x_5 + k_8x_6 + k_9x_6 - k_{10}x_5x_7 + k_{11}x_9 + k_{12}x_9, \\ \dot{x}_6 &= k_7x_4x_5 - k_8x_6 - k_9x_6, \\ \dot{x}_7 &= -k_{10}x_5x_7 + k_6x_8 + k_{11}x_9 - k_{29}x_7 + k_{35}x_{16}, \\ \dot{x}_8 &= k_4x_1x_4 - k_5x_8 - k_6x_8 - k_{30}x_8 + k_{36}x_{17}, \\ \dot{x}_9 &= k_{10}x_5x_7 - k_{11}x_9 - k_{12}x_9, \\ \dot{x}_{10} &= k_{14}x_{11} + k_{15}x_{11} - k_{13}x_{10}x_{12} - k_{16}x_{10}x_{13} + k_{17}x_{17} + k_{18}x_{17} + k_{25}x_1 - k_{31}x_{10}, \\ \dot{x}_{11} &= -k_{14}x_{11} - k_{15}x_{11} + k_{13}x_{10}x_{12} + k_{26}x_2 - k_{32}x_{11}, \\ \dot{x}_{12} &= k_{14}x_{11} - k_{13}x_{10}x_{12} + k_{21}x_{15} + k_{27}x_3 - k_{33}x_{12}, \\ \dot{x}_{13} &= k_{15}x_{11} - k_{16}x_{10}x_{13} - k_{19}x_{13}x_{14} + k_{20}x_{15} + k_{17}x_{17} + k_{24}x_{18} + k_{28}x_4 - k_{34}x_{13}, \\ \dot{x}_{14} &= -k_{19}x_{13}x_{14} + k_{20}x_{15} + k_{21}x_{15} - k_{22}x_{14}x_{16} + k_{23}x_{18} + k_{24}x_{18}, \\ \dot{x}_{15} &= k_{19}x_{13}x_{14} - k_{20}x_{15} - k_{21}x_{15}, \\ \dot{x}_{16} &= -k_{22}x_{14}x_{16} + k_{18}x_{17} + k_{23}x_{18} + k_{29}x_7 - k_{35}x_{16}, \\ \dot{x}_{17} &= k_{16}x_{10}x_{13} - k_{17}x_{17} - k_{18}x_{17} + k_{30}x_8 - k_{36}x_{17}, \\ \dot{x}_{18} &= k_{22}x_{14}x_{16} - k_{23}x_{18} - k_{24}x_{18}. \end{aligned}$$

This system has the following conserved amounts:

$$\begin{aligned} E_{tot} &= x_1 + x_2 + x_8 + x_{10} + x_{11} + x_{17}, \\ F_{tot} &= x_5 + x_6 + x_9, \\ F_{tot}^c &= x_{14} + x_{15} + x_{18}, \\ S_{tot} &= x_2 + x_3 + x_4 + x_6 + x_7 + x_8 + x_9 + x_{11} + x_{12} + x_{13} + x_{15} + x_{16} + x_{17} + x_{18}. \end{aligned}$$

**Creation of multistationarity in a two-site phosphorylation cycle.** We use the CRNT toolbox to obtain initial rate constants and total amounts for which the system admits multiple positive steady states. The output rate constants do not fulfill  $\alpha_1, \alpha_2, \alpha_3 > 0$  in each compartment independently. Hence, it is not possible to decide whether multistationarity arises due to shuttling or due to phosphorylation of two different sites.

Next we investigate the effect of changing the rate constants with respect to the existence of multistationarity for the same total amounts. We proceed by manually modifying the rates while keeping multistationarity and such that the sufficient conditions for the preclusion of multistationarity in a two-site phosphorylation cycle are satisfied in each compartment.

We end up with the following rate constants:

- Reaction rates in the nucleus:

$$\begin{array}{llllll} k_1 = 100 & k_2 = 2 & k_3 = 10 & k_4 = 80 & k_5 = 6 & k_6 = 6 \\ k_7 = 350 & k_8 = 3 & k_9 = 10 & k_{10} = 650 & k_{11} = 8 & k_{12} = 8. \end{array}$$

- Reaction rates in the cytoplasm:

$$\begin{array}{llllll} k_{13} = 300 & k_{14} = 1 & k_{15} = 10 & k_{16} = 50 & k_{17} = 1 & k_{18} = 1 \\ k_{19} = 350 & k_{20} = 30 & k_{21} = 190 & k_{22} = 150 & k_{23} = 2 & k_{24} = 20. \end{array}$$

- Shuttling rates:

$$\begin{array}{llllll} k_{25} = 10 & k_{26} = 30 & k_{27} = 70 & k_{28} = 30 & k_{29} = 1 & k_{30} = 10 \\ k_{31} = 450 & k_{32} = 20 & k_{33} = 20 & k_{34} = 25 & k_{35} = 10 & k_{36} = 100. \end{array}$$

This choice of rate constants fulfills that  $\alpha_1, \alpha_2, \alpha_3 > 0$  in the nucleus and in the cytoplasm (where in the later, indices of the rate constants in  $\alpha_*$  are shifted by 12). Therefore, with these rate constants, the two-site phosphorylation cycles in the nucleus and in the cytoplasm cannot have multiple positive steady states independently of each other.

The system with the shuttling reactions, however, does have the capacity for multistationarity. Specifically, if the total amounts are set to:

$$E_{tot} = 50, \quad S_{tot} = 100 \quad F_{tot} = 15 \quad F_{tot}^c = 21,$$

then the system has three positive steady states: two of them are stable and one is unstable. The positive steady states are the following:

$$\begin{aligned} SS_1 &= (1.89, 9.18, 0.62, 1.88, 0.01, 0.7, 25.11, 23.21, 14.28, 0.07, 13.38, 6.8, 0.04, 18.49, 1.15, 0.01, 2.28, 1.36) \\ SS_2 &= (6.45, 5.93, 0.1, 0.61, 0.01, 0.17, 35.4, 25.64, 14.82, 0.13, 9.33, 2.8, 0.03, 18.32, 0.8, 0.02, 2.52, 1.89) \\ SS_3 &= (0.37, 17.59, 5.96, 2.3, 0.17, 10.66, 0.6, 5.65, 4.16, 0.04, 25.8, 24.89, 0.06, 19.22, 1.72, 0.00044, 0.56, 0.06). \end{aligned}$$

Here  $SS_1$  is the unstable steady state.

**Rate constants to obtain seven steady states (for Figs. 4(B-D) in the main text).** Additionally, we have observed that, with specific choices of rate constants and total amounts, up to 7 steady states can be created in this system. For instance, consider the rate constants (used in the main text to create Figures 4(B-D)):

$$\begin{aligned} (k_1, \dots, k_{12}) &= (101, 2, 11, 79, 6, 6, 568, 3, 12, 1502, 8, 8), \\ (k_{13}, \dots, k_{24}) &= (210, 3, 34, 49, 1, 1, 344, 26, 187, 149, 1, 1), \\ (k_{25}, \dots, k_{36}) &= (10, 34, 7.5, 312.5, 0.1, 0.1, 44, 23, 2, 250, 0.1, 0.1), \end{aligned}$$

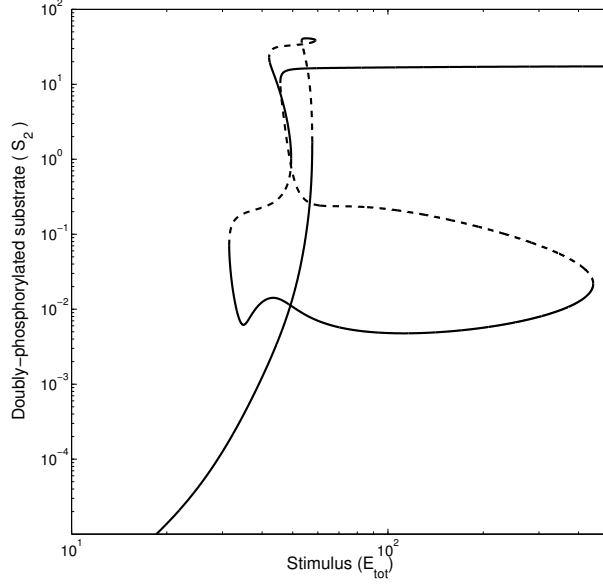


Figure 8: The steady state response curve of  $S_2$  as stimulus ( $E_{tot}$ ) varies. All other parameters are at baseline values. Stable state, solid line; unstable state, dashed line.

and the total amounts  $(E_{tot}, S_{tot}, F_{tot}, F_{tot}^c) = (57, 111, 15, 21)$ . This system has 7 steady states, 4 of which are stable:

$$\begin{aligned}
 SS_1 &= (18.27, 2.41, 0.04, 0.03, 5.05, 6.28, 0.01, 4.12, 3.67, 5.2, 1.45, 0.005, 0.21, 0.01, 0.002, 46.2, 25.61, 20.99) \\
 SS_2 &= (12.66, 1.2, 0.03, 0.17, 0.47, 3.11, 0.26, 14.67, 11.42, 3.4, 0.73, 0.004, 0.3, 0.01, 0.004, 33.77, 24.34, 20.99) \\
 SS_3 &= (13.01, 0.05, 0.0009, 0.23, 0.01, 0.09, 16.34, 19.9, 14.9, 2.96, 0.06, 0.003, 0.29, 0.02, 0.01, 17.14, 21.06, 20.1) \\
 SS_4 &= (13.66, 2.04, 0.004, 0.23, 0.004, 0.039, 35.84, 20.54, 14.96, 2.63, 3.95, 0.3, 0.22, 2.48, 0.84, 0.1, 14.18, 17.76) \\
 SS_5 &= (14.56, 3.53, 0.006, 0.22, 0.004, 0.03, 40.64, 20.63, 14.96, 2.49, 6.85, 0.56, 0.14, 6.54, 1.45, 0.03, 8.95, 13.01) \\
 SS_6 &= (4, 15.03, 0.4, 0.49, 0.27, 5.07, 0.38, 12.88, 9.65, 0.12, 23.78, 35.81, 0.2, 14.89, 4.88, 0.001, 1.19, 1.23) \\
 SS_7 &= (5.94, 11.14, 0.15, 0.5, 0.02, 0.43, 6.89, 19.51, 14.55, 0.12, 18.91, 31.22, 0.17, 14.86, 4.07, 0.002, 1.38, 2.07)
 \end{aligned}$$

The stable steady states are  $SS_1, SS_3, SS_5, SS_6$ .

As  $E_{tot}$  varies, the number of states changes as shown on a log-log scale in Figure 8, corresponding to the bifurcation diagram (Figure 4B in the main text, semi-log scale).

## B Software tools

Calculations to assess multistationarity were made using Mathematica (Wolfram Research, Inc., Mathematica, Version 7.0, Champaign, IL., 2010) and CRNT toolbox [20]. Bifurcation diagrams were computed using Oscill8 [32] and visualized with MATLAB (The MathWorks Inc., Natick, MA, R2011b). Figures in the main text were created using Adobe Illustrator (Versions CS3 and CS4. San Jose, California: Adobe Systems, Inc., 2011).

## References

- [1] Cheong R, Rhee A, Wang CJ, Nemenman I, Levchenko A (2011) Information Transduction Capacity of Noisy Biochemical Signaling Networks. *Science* 334: 354–358.
- [2] Toyoshima Y, Kakuda H, Fujita KA, Uda S, Kuroda S (2012) Sensitivity control through attenuation of signal transfer efficiency by negative regulation of cellular signaling. *Nature Communications* 3:1–8.
- [3] Balázsi G, van Oudenaarden A, Collins JJ (2011) Cellular decision making and biological noise: from microbes to mammals. *Cell* 144:910–925.
- [4] Pearlman, SM and Serber, Z and Ferrell Jr, JE (2011) A Mechanism for the Evolution of Phosphorylation Sites. *Cell* 147:934–946.
- [5] Ozbudak EM, Thattai M, Lim HN and Shraiman BI, van Oudenaarden A (2004) Multistability in the lactose utilization network of *Escherichia coli*. *Nature* 427:737–740.
- [6] Qiao L, Nachbar RB, Kevrekidis IG, Shvartsman SY (2007) Bistability and oscillations in the Huang-Ferrell model of MAPK signaling. *PLoS Comput Biol* 3:1819–1826.
- [7] Ferrell JE, Bhatt RR (1997) Mechanistic studies of the dual phosphorylation of mitogen-activated protein kinase. *J Biol Chem* 272:19008–19016.
- [8] Thomson M, Gunawardena J (2009) Unlimited multistability in multisite phosphorylation systems. *Nature* 460:274–277.
- [9] Fujioka A, Matsuda M, et al. (2006) Dynamics of the Ras/ERK MAPK cascade as monitored by fluorescent probes. *J Biol Chem* 281:8917–8926.
- [10] Lidke DS, Lenormand P, et al. (2010) ERK nuclear translocation is dimerization-independent but controlled by the rate of phosphorylation. *Proc Natl Acad Sci USA* 107:3092–3102.
- [11] Harrington HA, Komorowski M, Beguerisse-Díaz M, Ratto GM, Stumpf MPH (2012) Mathematical modeling reveals the functional implications of the different nuclear shuttling rates of Erk1 and Erk2. *Phys Biol* 9:036001.
- [12] Kholodenko BN, Hancock JF, Kolch W (2010) Signaling ballet in space and time. *Nat Rev Mol Cell Biol* 11:414–426.
- [13] Santos SDM, Wollman R, Meyer T, Ferrell JE (2012) Spatial positive feedback at the onset of mitosis. *Cell* 149:1500–1513.
- [14] Feynman RP (1996) Feynman Lectures on Computation (Perseus Books).
- [15] Bhalla US (2011) Trafficking motifs as the basis of two-compartment signaling systems to form multiple stable states. *Biophys J* 101:21–32.
- [16] Goldbeter A, Koshland DE (1981) An amplified sensitivity arising from covalent modification in biological systems. *Proc Natl Acad Sci USA* 78:6840–6844.
- [17] Goldbeter A, Koshland DE (1984) Ultrasensitivity in biochemical systems controlled by covalent modification. Interplay between zero-order and multistep effects. *J Biol Chem* 259: 14441–14447.
- [18] Bass H, Connell EH, Wright D. (1982) The Jacobian conjecture: reduction of degree and formal expansion of the inverse. *Bull Amer Math Soc* 7: 287–330.
- [19] Pantea C, Koepl H, Craciun G. (2012) Global injectivity and multiple equilibria in uni- and bi-molecular reaction networks. *Discrete and Continuous Dynamical Systems - Series B* 17:6.
- [20] Ellison P, Feinberg M, Ji H (2012) Chemical Reaction Network Toolbox. Available at <http://www.chbmeng.ohio-state.edu/~feinberg/crntwin/>.
- [21] Feliu E, Wiuf C (2012) Preclusion of switch behavior in reaction networks with mass-action kinetics. *Applied Math Comput*. <http://dx.doi.org/10.1016/j.amc.2012.07.048>.
- [22] Radhakrishnan K, Oliver JM, et al. (2009) Sensitivity analysis predicts that the ERK-pMEK interaction regulates ERK nuclear translocation. *Systems biology*, 3:329–341.

- [23] Markevich NI, Hoek JB, Kholodenko BN (2004) Signaling switches and bistability arising from multisite phosphorylation in protein kinase cascades. *J Cell Biol* 164:353–359.
- [24] Wang L, Sontag ED (2008) On the number of steady states in a multiple futile cycle. *J Math Biol* 57:29–52.
- [25] Shankaran H, Wiley HS, et al. (2009) Rapid and sustained nuclear-cytoplasmic ERK oscillations induced by epidermal growth factor. *Mol Syst Biol* 5:332.
- [26] Kholodenko BN, Birtwistle MR (2009) Four-dimensional dynamics of MAPK information processing systems. *Wiley Interdiscip Rev Syst Biol Med* 1:28–44.
- [27] Costa M, Ratto GM, et al. (2006) Dynamic regulation of ERK2 nuclear translocation and mobility in living cells. *J Cell Sci* 119:4952–4963.
- [28] von Kriegsheim A, Kolch W, et al. (2009) Cell fate decisions are specified by the dynamic ERK interactome. *Nature* 11:1458–1464.
- [29] Maynard Smith J, Szathmary E (1997) *The Major Transitions in Evolution* (Oxford Univ Press).
- [30] McGuffee SR, Elcock AH (2010) Diffusion, Crowding & Protein Stability in a Dynamic Molecular Model of the Bacterial Cytoplasm. *PLoS Comp Biol* 6:e1000694.
- [31] Feliu E, Wiuf C (2012) Enzyme sharing as a cause of multistationarity in signaling systems. *J R Soc Interface* 9:1224–1232.
- [32] Conrad E (2008) Oscill8. Available at <http://oscill8.sourceforge.net/doc/>.